

Increased Heat Transport in Ultra-Hot Jupiter Atmospheres Through H₂ Dissociation/Recombination

TAYLOR J. BELL^{1,*} AND NICOLAS B. COWAN^{1,2,*}

¹*Department of Physics, McGill University, 3600 rue University, Montréal, QC H3A 2T8, Canada*

²*Department of Earth & Planetary Sciences, McGill University, 3450 rue University, Montréal, QC H3A 0E8, Canada*

(Received 2018 January 30; Revised 2018 April 04; Accepted 2018 April 07)

Submitted to ApJL

ABSTRACT

A new class of exoplanets is beginning to emerge: planets whose dayside atmospheres more closely resemble stellar atmospheres as most of their molecular constituents dissociate. The effects of the dissociation of these species will be varied and must be carefully accounted for. Here we take the first steps towards understanding the consequences of dissociation and recombination of molecular hydrogen (H₂) on atmospheric heat recirculation. Using a simple energy balance model with eastward winds, we demonstrate that H₂ dissociation/recombination can significantly increase the day–night heat transport on ultra-hot Jupiters (UHJs): gas giant exoplanets where significant H₂ dissociation occurs. The atomic hydrogen from the highly irradiated daysides of UHJs will transport some of the energy deposited on the dayside towards the nightside of the planet where the H atoms recombine into H₂; this mechanism bears similarities to latent heat. Given a fixed wind speed, this will act to increase the heat recirculation efficiency; alternatively, a measured heat recirculation efficiency will require slower wind speeds after accounting for H₂ dissociation/recombination.

Keywords: planets and satellites: atmospheres — planets and satellites: gaseous planets — methods: analytical — methods: numerical

1. INTRODUCTION

Most gas giant exoplanets have atmospheres dominated by molecular hydrogen (H₂). However, on planets where the temperature is sufficiently high, a significant fraction of the H₂ will thermally dissociate; one may call these planets ultra-hot Jupiters (UHJs). Only a handful of known planets have dayside temperatures this high, but the TESS mission is expected to discover hundreds more as it includes many early-type stars (George Zhou, private communication 2017). These UHJs are an interesting intermediate between stars and cooler planets, and they will allow for useful tests of atmospheric models.

At these star-like temperatures, the H[−] bound-free and free-free opacities should play an important role in the continuum atmospheric opacity which has recently been detected in dayside secondary eclipse spectra (Bell et al. 2017; Arcangeli et al. 2018). These recently reported detections of H[−] opacity provide evidence that H₂ is dissociating in the atmospheres of gas giants at this temperature range. However, the thermodynamical effects of H₂ dissociation/recombination have yet to be explored.

Both theoretically (e.g. Perez-Becker & Showman 2013; Komacek & Showman 2016) and empirically (e.g. Zhang et al. 2018; Schwartz et al. 2017), we expect the day–night temperature contrast on hot Jupiters to increase with increasing stellar irradiation; temperature gradients $\gtrsim 1000$ K can be expected for UHJs. As temperatures vary drastically between day and night, the local thermal equilibrium (LTE) H₂ dissociation fraction will also vary. The recombination of H into H₂ is a remarkably exothermic process, releasing

Corresponding author: Taylor J. Bell
taylor.bell@mail.mcgill.ca

* McGill Space Institute; Institute for Research on Exoplanets;
Centre for Research in Astrophysics of Quebec

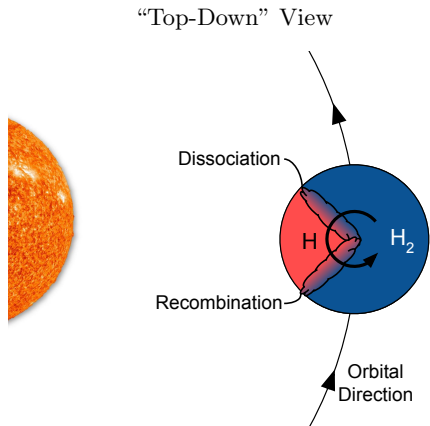


Figure 1. A cartoon showing a “top-down” view of the expected dissociation and recombination of H_2 on an ultra-hot Jupiter (UHJ). The orbital direction and the direction of winds on the planet are indicated with black arrows.

$q = 2.14 \times 10^8 \text{ J kg}^{-1}$ (Dean 1999); this is $100\times$ more potent than the latent heat of condensation for water. For reference, latent heat is responsible for approximately half of the heat recirculation on Earth ($L/(c_p \Delta T) \sim 1$), while the effect of H_2 dissociation/recombination should be even stronger for UHJs ($q/(c_p \Delta T) \sim 10^2$).

Building on this intuition, we might expect that H will recombine into H_2 as gas carried by winds flows eastward from the sub-stellar point, significantly heating the eastern hemisphere of the planet. As the gas continues to flow around to the dayside, the H_2 will again dissociate and significantly cool the western hemisphere. A cartoon depicting this layout is shown in Figure 1. If unaccounted for while modelling a phasecurve, this may manifest itself as an “unphysically” large eastward offset as was previously reported for WASP-12b (Cowan et al. 2012).

A large number of circulation models have been developed for studying exoplanet atmospheres, ranging from simple energy balance models (e.g. Cowan & Agol 2011) to more advanced general circulation models (e.g. Showman et al. 2009; Rauscher & Menou 2010; Amundsen et al. 2014; Zhang & Showman 2017; Heng & Kitzmann 2017; Dobbs-Dixon & Cowan 2017). To our knowledge, however, no published general circulation models account for the cooling/heating due to the energies of H_2 dissociation/recombination (although some planet formation models do account for this, e.g. Berardo et al. 2017). Here we aim to qualitatively explore the effects of H_2 dissociation/recombination using a simple energy balance model adapted from that described by Cowan & Agol (2011), using code based on that implemented by Schwartz et al. (2017). We leave it to those with more

advanced circulation models to explore this problem in a more rigorous and quantitative manner.

2. ENERGY TRANSPORT MODEL

2.1. Heating Terms

First, let ϵ be the energy per unit area of a parcel of gas. Ignoring H_2 dissociation/recombination and any internal heat sources, and assuming the gas parcel cools radiatively, energy conservation gives

$$\frac{d\epsilon}{dt} = F_{\text{in}} - F_{\text{out}},$$

with F_{in} and F_{out} given by

$$F_{\text{in}} = (1 - A_B) F_* \sin \theta \max(\cos \Phi(t), 0),$$

$$F_{\text{out}} = \sigma T^4.$$

The planet’s Bond albedo is given by A_B , θ is the colatitude of the gas parcel, T is the temperature of the gas parcel, and σ is the Stefan-Boltzmann constant. The incoming stellar flux is given by $F_* = \sigma T_{*,\text{eff}}^4 (R_*/a)^2$, where $T_{*,\text{eff}}$ is the stellar effective temperature, R_* is the stellar radius, and a is the planet’s semi-major axis. The stellar hour angle, $\Phi(t)$, incorporates both advection and planetary rotation.

In order to include H_2 dissociation/recombination, we add a new term accounting for the energy flux from these effects. This can be done with

$$\frac{d\epsilon}{dt} = F_{\text{in}} - F_{\text{out}} - \frac{d\mathbb{Q}}{dt}, \quad (1)$$

where the energy per unit area stored by H_2 dissociation is given by

$$\mathbb{Q} = q \chi_{\text{H}} \Sigma,$$

where Σ is the mass per unit area of H and H_2 in the parcel of gas (in kg m^{-2}), $q = 2.14 \times 10^8 \text{ J kg}^{-1}$ is the H_2 bond dissociation energy per unit mass at 0K, and χ_{H} is the dissociation fraction of the gas. $\chi_{\text{H}} = 1$ means the gas is completely dissociated (all atomic). Assuming the gas parcel is in hydrostatic equilibrium, we can use

$$\Sigma = \int_{z_0}^{\infty} \rho(z) dz = (P_0/g)$$

where z_0 is some reference height, P_0 is the atmospheric pressure corresponding to z_0 , and ρ is the density of the gas. This then allows us to rewrite \mathbb{Q} as

$$\mathbb{Q} = (P_0/g) q \chi_{\text{H}}.$$

The time derivative of \mathbb{Q} is then

$$\frac{d\mathbb{Q}}{dt} = (P_0/g) q \frac{d\chi_{\text{H}}}{dt} = (P_0/g) q \left. \frac{d\chi_{\text{H}}}{dT} \right|_T \frac{dT}{dt}, \quad (2)$$

where we have assumed the gas parcel's P_0/g remains constant, and where we have made use of the chain rule to expand $d\chi_H/dt$.

We model the LTE H₂ dissociation fraction by solving the Saha equation as stated in Appendix A of [Berardo et al. \(2017\)](#) for χ_H , assuming the atmosphere consists of only H and H₂:

$$\chi_H(P, T) = \frac{n_H}{n_H + n_{H_2}} = \frac{2}{1 + \sqrt{1 + 4Y}}, \quad (3)$$

where n_H and n_{H_2} are the number densities of H and H₂,

$$Y = \frac{T^{-3/2} \exp(q/2m_H k_B T) P}{2(\pi m_H)^{3/2} k_B^{5/2} h^{-3} \Theta_{\text{rot}}},$$

where m_H is the mass of the hydrogen atom, k_B is the Boltzmann constant, h is the Planck constant, $\Theta_{\text{rot}} = 85.4 \text{ K}$ is rotational temperature of H₂ ([Hill 1986](#)), P is the gas pressure, and T is the temperature of the gas (in K). The LTE dissociation fraction is plotted in the top panel of Figure 2.

We can then find $d\chi_H/dT$ using the chain rule:

$$\frac{d\chi_H}{dT} = \frac{d\chi_H}{dY} \frac{dY}{dT}.$$

After some simplification, we then determine

$$\frac{d\chi_H}{dT} = \frac{\chi_H^2 Y \left(\frac{3}{2} T^{-1} + (q/2m_H k_B) T^{-2} \right)}{\sqrt{1 + 4Y}}. \quad (4)$$

To a good degree of accuracy, Equations (3) and (4) can be approximated at $P = 0.1 \text{ bar}$ using

$$\chi_H(0.1 \text{ bar}, T) = \frac{1}{2} \left(1 + \operatorname{erf} \left(\frac{T - \mu}{\sigma \sqrt{2}} \right) \right) \quad (5)$$

and

$$\frac{d\chi_H(0.1 \text{ bar}, T)}{dT} = \frac{1}{\sigma \sqrt{2\pi}} e^{-(T-\mu)^2/2\sigma^2} \quad (6)$$

where $\sigma = 471 \text{ K}$ and $\mu = 3318 \text{ K}$, and erf is the error function; this approximation offers a 70% increase in computation speed. It should be noted that we assume that this H₂ dissociation/recombination occurs instantaneously since the timescale in the temperature regime of UHJs at 0.1 bar is $\sim 10^{-3} \text{ s}$ ([Rink 1962](#); [Shui 1973](#)).

2.2. Thermal Energy

We assume that the planet's energy is stored entirely as thermal energy, as is done in other simple energy

balance models (e.g. [Cowan & Agol 2011](#); [Pierrehumbert 2010](#)). This assumption means

$$\begin{aligned} \frac{d\epsilon}{dt} &= \frac{d}{dt}(c_p T \Sigma) = \frac{d}{dt} \left((P_0/g) c_p T \right) \\ &= (P_0/g) \left(c_p \frac{dT}{dt} + T \frac{dc_p}{dt} \right) \\ &= (P_0/g) \frac{dT}{dt} \left(c_p + T \frac{dc_p}{dT} \Big|_T \right). \end{aligned} \quad (7)$$

where c_p is the specific heat capacity of the gas, we have again assumed the gas parcel's P_0/g remains constant, and we have used the chain rule to expand dc_p/dt .

The specific heat capacity of the gas will change as a function of temperature due to the slightly different values for H and H₂ as well as the variations in the specific heat capacity of H₂ as a function of temperature ([Chase 1998](#)); any model properly accounting for H₂ dissociation should account for this effect. In our model, we assume the atmosphere is made entirely of hydrogen and model the specific heat capacity of the gas by assuming it is well mixed so that

$$c_p = c_{p,H} \chi_H + c_{p,H_2} (1 - \chi_H),$$

where both χ_H and c_{p,H_2} are functions of temperature. The temperature derivative of c_p is then given by

$$\frac{dc_p}{dT} \Big|_T = (c_{p,H} - c_{p,H_2}) \frac{d\chi_H}{dT} \Big|_T.$$

2.3. Putting Everything Together

Putting together Equations (1), (2) and (7), we get

$$\begin{aligned} F_{\text{in}} - F_{\text{out}} - (P_0/g) \frac{dT}{dt} \left(q \frac{d\chi_H}{dT} \Big|_T \right) \\ = (P_0/g) \frac{dT}{dt} \left(c_p + T \frac{dc_p}{dT} \Big|_T \right). \end{aligned}$$

After solving for dT/dt , we find

$$\frac{dT}{dt} = (F_{\text{in}} - F_{\text{out}}) (P_0/g)^{-1} \left(c_p + T \frac{dc_p}{dT} \Big|_T + q \frac{d\chi_H}{dT} \Big|_T \right)^{-1}.$$

Finally, a gas cell can then be updated using

$$\Delta T = \frac{\Delta t (F_{\text{in}} - F_{\text{out}})}{(P_0/g) \left(c_p + T \frac{dc_p}{dT} \Big|_T + q \frac{d\chi_H}{dT} \Big|_T \right)}. \quad (8)$$

Note that the entire sum in the denominator can instead be thought of as the specific heat capacity of a gas comprised of a mixture of H and H₂ in thermal equilibrium. The relative importance of the terms in this sum are shown in the bottom two panels of Figure 2.

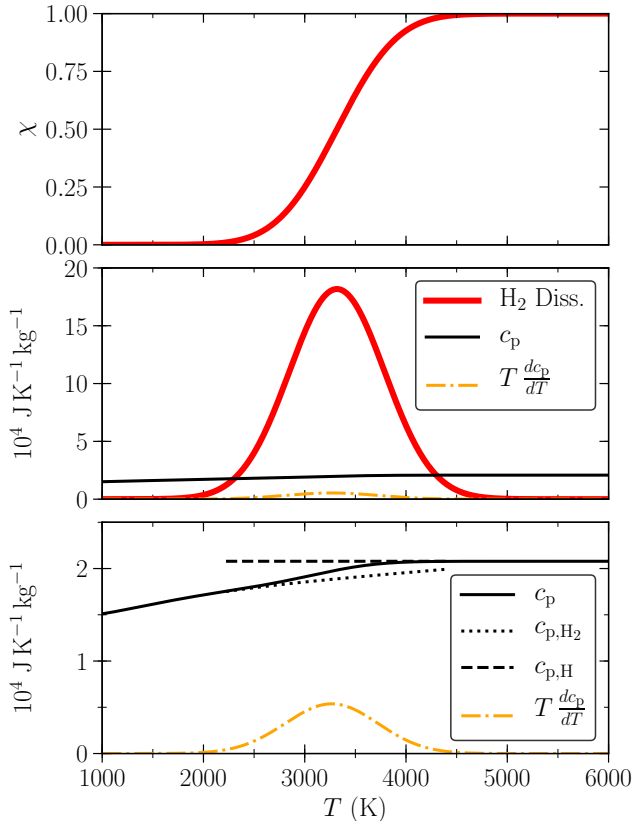


Figure 2. *Top:* The LTE dissociation fraction of H_2 in a parcel of gas. *Middle:* A demonstration of the relative importance of the H_2 dissociation/recombination term in Equation (8). For $2300 \lesssim T \lesssim 4300$, the energy absorbed by H_2 dissociation is greater than the energy stored as heat. Typical hot Jupiters are too cool to be affected by H_2 dissociation/recombination, but these processes should dominate on UHJs. *Bottom:* An inset showing the specific heat capacity of a gas composed of H and H_2 in LTE (the same black line from the middle panel), the specific heat capacities of H and H_2 where they are able to exist in equilibrium, and the additional $T(dc_p/dT)$ term. All panels assume a pressure of 0.1 bar.

3. SIMULATED OBSERVATIONS AND QUALITATIVE TRENDS

We now explore the effects of this new term in the differential equation governing the temperature of a gas cell. For this purpose, we create a latitude+longitude HEALPix grid where each parcel’s temperature is updated using Equation (8) with code based on that developed by Schwartz et al. (2017).

While Cowan & Agol (2011) were able to explore their model using dimensionless quantities, our updated model requires that we use dimensioned variables. We therefore adopt the values of the first discovered UHJ, WASP-12b (Hebb et al. 2009). In particular, we set $R_p = 1.90 R_J$, $a = 0.0234 \text{ AU}$, $M_p = 1.470 M_J$,

$T_{*,\text{eff}} = 6360 \text{ K}$, $R_* = 1.657 R_\odot$, $P = 1.0914203 \text{ days}$ (Collins et al. 2017) and $A_B = 0.27$ (Schwartz et al. 2017). We have also assumed a photospheric pressure of 0.1 bar, the approximate pressure probed by NIR observations of WASP-12b (Stevenson et al. 2014), which gives a radiative timescale of a few hours (similar to the observed timescales for eccentric hot Jupiters, e.g. Lewis et al. 2013; de Wit et al. 2016). Wind speeds for WASP-12b have not been directly measured, but typical values for hot Jupiters are on the order of 1 km s^{-1} (e.g. Koll & Komacek 2017); for that reason, we focus on wind speeds around this order of magnitude.

First, let’s explore the effects of H_2 dissociation/recombination at a spatially resolved scale. Figure 3 shows temperature and H_2 dissociation maps for three different wind speeds. In the limit of infinite wind speeds, there will be no temperature gradients and H_2 dissociation/recombination will not play a role. In the limit of an atmosphere in radiative equilibrium (wind speed = 0), there will be no variation in the temperature of a parcel and H_2 dissociation/recombination will play no role. Outside of these two unphysical limits, H_2 dissociation/recombination will always be occurring somewhere on UHJs.

We now consider phasecurve observations — this requires that we convolve the planet map with a visibility kernel at each orbital phase (Cowan et al. 2013), which acts as a low-pass filter. Figure 4 shows model phasecurves for three wind speed; this figure shows that H_2 dissociation/recombination can have a significant effect. At a constant wind speed, the first obviously affected observable when accounting for dissociation/recombination is the increased offset of the peak in the phasecurve towards the east (the same direction as the prescribed wind). Another affected observable is the amplitude of the phase variations which is reduced when H_2 dissociation/recombination is included. Also, a Fourier decomposition shows that nearly all of the power in the phasecurves accounting for H_2 dissociation/recombination is in the first and second order Fourier series terms ($1f_{\text{orb}}$ and $2f_{\text{orb}}$). Finally, Figure 5 shows the trends in phase offset and nightside temperature for two wind speeds, both accounting for and neglecting H_2 dissociation/recombination.

4. MODEL ASSUMPTIONS

With simplistic models, many important effects are necessarily swept under the rug. Here we aim to lift up the rug and shine a light on our assumptions to aid future work. While many of these assumptions will change the quantitative effects of H_2 dissociation/recombination, we expect that the overall qualitative im-

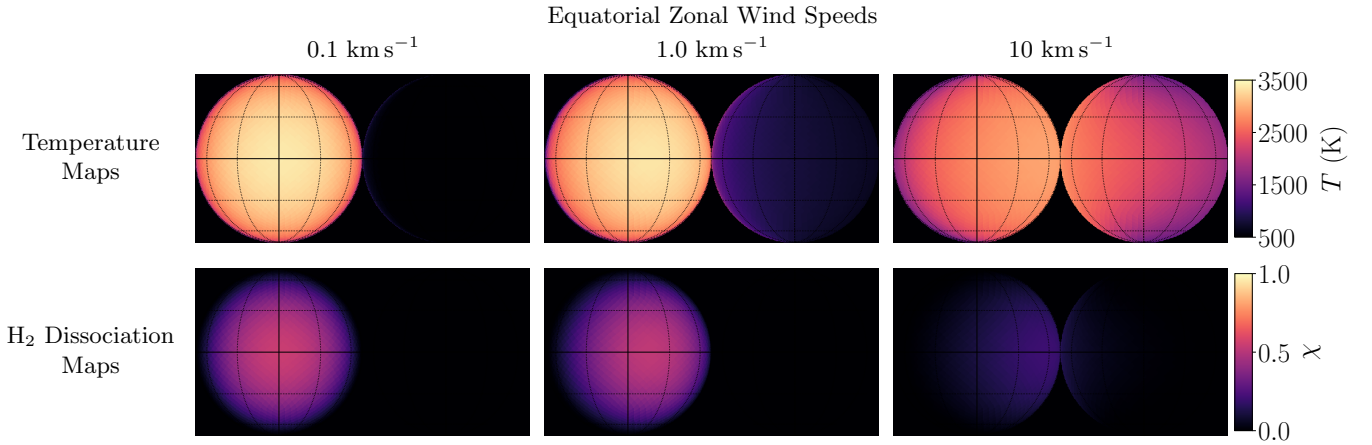


Figure 3. Planetary maps, showing temperature and H₂ dissociation fraction, assuming different eastward zonal wind speeds. The dayside hemisphere is shown on the left side of each map with north at the top.

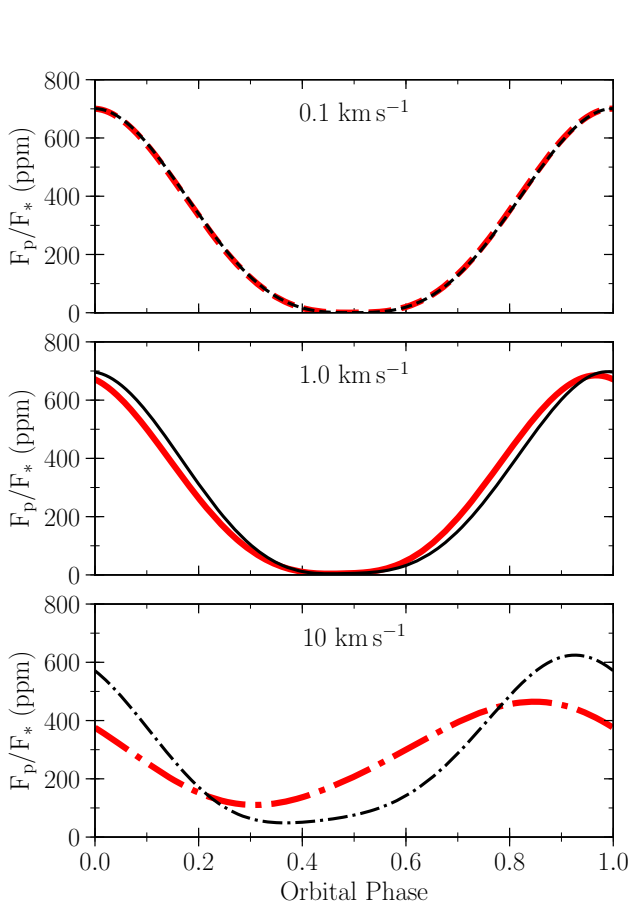


Figure 4. Model bolometric phasecurves assuming different eastward zonal wind velocities, ignoring eclipses and transits. The thick, red lines show the expected phasecurve accounting for H₂ dissociation/recombination, while the thinner, black models neglect these processes. Secondary eclipse would occur at a phase of 0.0, while a transit would occur at 0.5.

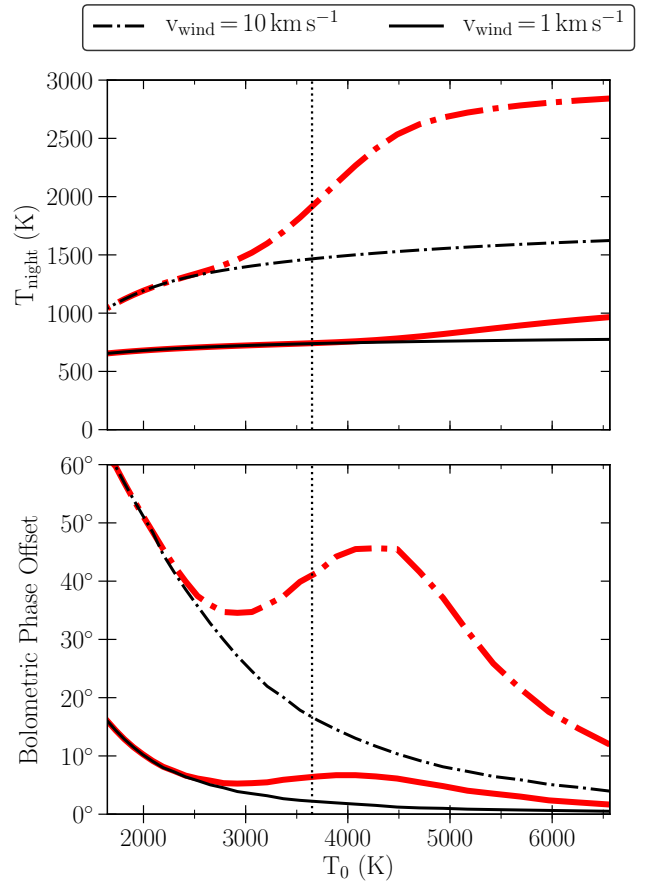


Figure 5. A figure showing the trends in nightside apparent temperature and phase offset as a function of irradiation temperature ($T_0 \equiv T_{*,\text{eff}} \sqrt{R_*/a}$), given theoretical bolometric phasecurve measurements. Thick, red lines show models including H₂ dissociation/recombination for WASP-12b, while thin, black lines show models neglecting these effects. Models sharing the same wind speed share linestyles, and all models assume a Bond albedo of 0.3 (which is typical for hot Jupiters; Zhang et al. 2018; Schwartz et al. 2017). A vertical dotted line shows the location of WASP-12b.

pact of increased heat recirculation will be robust to these assumptions.

One important piece of physics that we have ignored (beyond a simple assumption of a 0.1 bar photosphere) is atmospheric opacity. As [Dobbs-Dixon & Cowan \(2017\)](#) demonstrated, variations in opacity sources as a function of longitude can change the depth of the photosphere by an order of magnitude or more. Changing the H_2 dissociation fraction will change the importance of H^- as an opacity source, and other standard opacity sources (e.g. H_2O and CO) will also likely be important, especially towards the cooler nightside. The insignificant detection of H_2O on the dayside of WASP-12b ([Steven-son et al. 2014](#)) but significant detection in the planet’s transmission spectrum ([Kreidberg et al. 2015](#)) clearly demonstrates that opacity sources should be expected to change on UHJs. Several of the standard molecular opacity sources will also overlap with the far broader H^- absorption, which complicates a definitive detection of H^- using broadband photometry, such as with *Spitzer*/IRAC. The formation of clouds on the nightside of the planet would further complicate the interpretation of observed phasecurves, increasing the albedo of the west terminator while also insulating the nightside. While we have accounted for variations in the radiative timescale as a function of temperature, we have not accounted for changes due to varying opacity sources.

Additionally, as we have assumed all photons are emitted at a 0.1 bar photosphere, the effects of the atmosphere’s T-P profile have been neglected. As the H_2 dissociation fraction has a fairly weak dependence on gas pressure, the bulk of vertical variations in the H_2 dissociation fraction will likely be controlled by the vertical temperature gradient. Due to the lower density of the dissociated gas, one may expect vertical advection on UHJs where temperature decreases with altitude. Interestingly, however, observations of most UHJs are best explained by atmospheres with thermal inversions ([Arcangeli et al. 2018](#); [Evans et al. 2017](#)) or at least approximately isothermal profiles on the dayside ([Crossfield et al. 2012](#); [Cowan et al. 2012](#)). Any non-isothermal T-P profile will alter the specifics of how efficiently heat is redistributed across the planet as different layers in a gas column will dissociate/recombine at different locations. Also, as we have neglected atmospheric opacity, we have assumed that each gas parcel emits as a blackbody with a single temperature.

Further, due to the changing scale height of the atmosphere at different latitudes and longitudes due to changes in temperature and H_2 dissociation fraction, there will likely be a tendency for gas to flow away from the sub-stellar point both zonally and meridionally. This

is not accounted for in our toy model and would require a general circulation model. Instead, we have chosen eastward winds as they are predicted, and seen, for most hot Jupiters (e.g. [Showman & Guillot 2002](#); [Zhang et al. 2018](#)), although there are some exceptions (e.g. [Dang et al. 2018](#)). Similarly, our assumption of solid-body atmospheric rotation is clearly an over simplification which will need to be addressed in future work. Our model is also unable to predict the wind speeds of UHJs which would require the implementation of various drag sources, such as magnetic drag which [Menou \(2012\)](#) suggests will dominate at these high temperatures.

Also, we have assumed all heating is due to H_2 dissociation and radiation from the host star, neglecting other heat sources such as residual heat from formation (which should be negligible for planets older than 1 Gyr; [Burrows et al. 2006](#)) as well as tidal, viscous, and ohmic heating. We have also neglected the presence of helium which will partially dilute the strength of H_2 dissociation/recombination as only $\sim 80\%$ of the atmosphere will be hydrogen. Finally, we have assumed that the planet has a uniform albedo which will not be the case in general (e.g. [Esteves et al. 2013](#); [Demory et al. 2013](#); [Angerhausen et al. 2015](#); [Parmentier et al. 2016](#)).

5. DISCUSSION AND CONCLUSIONS

A new class of exoplanets is beginning to emerge: planets whose dayside atmospheres resemble stellar atmospheres as their molecular constituents thermally dissociate. The impacts of this dissociation will be varied and must be carefully accounted for. Here we have shown that the dynamical dissociation and recombination of H_2 will play an important role in the heat recirculation of ultra-hot Jupiters. In the atmospheres of ultra-hot Jupiters, significant H_2 dissociation occurs on the highly irradiated dayside, absorbing some of the incident stellar energy and transporting it towards the nightside of the planet where the gas recombines. Given a fixed wind speed, this will act to increase the heat recirculation efficiency; alternatively, a measured heat recirculation efficiency will require slower wind speeds once H_2 dissociation/recombination has been accounted for.

Both theoretically and observationally, it has been shown that increasing irradiation tends to lead to poorer heat recirculation (e.g. [Komacek & Showman 2016](#); [Schwartz et al. 2017](#)). However, there are a few notable exceptions to this rule at high temperatures. Recently, [Zhang et al. \(2018\)](#) reported a heat recirculation efficiency of $\varepsilon \sim 0.2$ for the UHJ WASP-33b which is far higher than would be predicted by theoretical and observational trends. WASP-12b may also possess an

unusually high heat recirculation efficiency and exhibit a greater phase offset than would be expected from simple heat advection¹ (Cowan et al. 2012). However, the power in the second order Fourier series terms from H₂ dissociation/recombination seems to make the phase-curve more sharply peaked and does not seem to be able to explain the double-peaked phasecurve seen for WASP-12b by Cowan et al. (2012). Also, while Arcangeli et al. (2018) find evidence of H₂ dissociation/recombination in the atmosphere of WASP-18b, Maxted et al. (2013) finds the planet has minimal day–night heat recirculation. Given the expected increase in heat recirculation due to H₂ dissociation/recombination, this suggests that WASP-18b has only moderate winds and/or

is too cool for these processes to play a strong role in the heat recirculation of this planet. Finally, near-infrared observations of KELT-9b, the hottest UHJ currently known (Gaudi et al. 2017), could provide a fantastic test of this theory in the very high temperature regime.

T.J.B. acknowledges support from the McGill Space Institute Graduate Fellowship and from the FRQNT through the Centre de recherche en astrophysique du Québec. The atmospheric model we use in this work is based upon code originally developed by Diana Jovmir and Joel Schwartz. We also thank Gabriel Marleau and Ian Dobbs-Dixon for their helpful insights. We have also made use of free and open-source software provided by the Python, SciPy, and Matplotlib communities.

REFERENCES

- Amundsen, D. S., Baraffe, I., Tremblin, P., et al. 2014, *A&A*, 564, A59
- Angerhausen, D., DeLarme, E., & Morse, J. A. 2015, *PASP*, 127, 1113
- Arcangeli, J., Desert, J.-M., Line, M. R., et al. 2018, *ArXiv e-prints*, arXiv:1801.02489
- Bell, T. J., Nikolov, N., Cowan, N. B., et al. 2017, *ApJL*, 847, L2
- Berardo, D., Cumming, A., & Marleau, G.-D. 2017, *ApJ*, 834, 149
- Burrows, A., Sudarsky, D., & Hubeny, I. 2006, *ApJ*, 650, 1140
- Chase, M. W. 1998, *J. Phys. Chem. Ref. Data*, Monograph 9, 1
- Collins, K. A., Kielkopf, J. F., & Stassun, K. G. 2017, *AJ*, 153, 78
- Cowan, N. B., & Agol, E. 2011, *ApJ*, 729, 54
- Cowan, N. B., Fuentes, P. A., & Haggard, H. M. 2013, *MNRAS*, 434, 2465
- Cowan, N. B., Machalek, P., Croll, B., et al. 2012, *ApJ*, 747, 82
- Crossfield, I. J. M., Barman, T., Hansen, B. M. S., Tanaka, I., & Kodama, T. 2012, *ApJ*, 760, 140
- Dang, L., Cowan, N. B., Schwartz, J. C., et al. 2018, *ArXiv e-prints*, arXiv:1801.06548
- de Wit, J., Lewis, N. K., Langton, J., et al. 2016, *ApJL*, 820, L33
- Dean, J. 1999, *Langes handbook of chemistry*, 36
- Demory, B.-O., de Wit, J., Lewis, N., et al. 2013, *ApJL*, 776, L25
- Dobbs-Dixon, I., & Cowan, N. B. 2017, *ApJL*, 851, L26
- Esteves, L. J., De Mooij, E. J. W., & Jayawardhana, R. 2013, *ApJ*, 772, 51
- Evans, T. M., Sing, D. K., Kataria, T., et al. 2017, *Nature*, 548, 58
- Gaudi, B. S., Stassun, K. G., Collins, K. A., et al. 2017, *Nature*, 546, 514
- Hebb, L., Collier-Cameron, A., Loeillet, B., et al. 2009, *ApJ*, 693, 1920
- Heng, K., & Kitzmann, D. 2017, *ApJS*, 232, 20
- Hill, T. L. 1986, *An Introduction to Statistical Thermodynamics* (Dover, New York)
- Koll, D. D. B., & Komacek, T. D. 2017, *ArXiv e-prints*, arXiv:1712.07643
- Komacek, T. D., & Showman, A. P. 2016, *ApJ*, 821, 16
- Kreidberg, L., Line, M. R., Bean, J. L., et al. 2015, *ApJ*, 814, 66
- Lewis, N. K., Knutson, H. A., Showman, A. P., et al. 2013, *ApJ*, 766, 95
- Maxted, P. F. L., Anderson, D. R., Doyle, A. P., et al. 2013, *MNRAS*, 428, 2645
- Menou, K. 2012, *ApJ*, 745, 138
- Parmentier, V., Fortney, J. J., Showman, A. P., Morley, C., & Marley, M. S. 2016, *ApJ*, 828, 22
- Perez-Becker, D., & Showman, A. P. 2013, *ApJ*, 776, 134
- Pierrehumbert, R. T. 2010, *Principles of Planetary Climate*
- Rauscher, E., & Menou, K. 2010, *ApJ*, 714, 1334

¹ Depending on the decorrelation method used to reduce the *Spitzer*/IRAC data for WASP-12b, the planet either has $\varepsilon \sim 0$ or $\varepsilon \sim 0.5$ (Cowan et al. 2012; Schwartz et al. 2017); although the former is the preferred model, further observations are critical to definitively choose between these values and test the predictions made in this article.

- Rink, J. P. 1962, JChPh, 36, 262
- Schwartz, J. C., Kashner, Z., Jovmir, D., & Cowan, N. B. 2017, ApJ, 850, 154
- Showman, A. P., Fortney, J. J., Lian, Y., et al. 2009, ApJ, 699, 564
- Showman, A. P., & Guillot, T. 2002, A&A, 385, 166
- Shui, V. H. 1973, JChPh, 58, 4868
- Stevenson, K. B., Bean, J. L., Madhusudhan, N., & Harrington, J. 2014, ApJ, 791, 36
- Zhang, M., Knutson, H. A., Kataria, T., et al. 2018, AJ, 155, 83
- Zhang, X., & Showman, A. P. 2017, ApJ, 836, 73